THE JOURNAL OF BIOLOGICAL CHEMISTRY VOL. 291, NO. 21, pp. 11407–11419, May 20, 2016

The Thumb Domain Mediates Acid-sensing Ion Channel Desensitization*

Received for publication, November 6, 2015, and in revised form, March 24, 2016 Published, JBC Papers in Press, March 25, 2016, DOI 10.1074/jbc.M115.702316

Aram J. Krauson[‡] **and Marcelo D. Carattino**[‡§1]

From the [‡]*Renal-Electrolyte Division, Department of Medicine, and* [§]*Department of Cell Biology, University of Pittsburgh, Pittsburgh, Pennsylvania 15261*

Acid-sensing ion channels (ASICs) are cation-selective proton-gated channels expressed in neurons that participate in diverse physiological processes, including nociception, synaptic plasticity, learning, and memory. ASIC subunits contain intracellular N and C termini, two transmembrane domains that constitute the pore, and a large extracellular loop with defined domains termed the finger, β-ball, thumb, palm, and knuckle. Here we examined the contribution of the finger, β-ball, and thumb domains to activation and desensitization through the analysis of chimeras and the assessment of the effect of covalent modification of introduced Cys at the domain-domain interfaces. Our studies with ASIC1a-ASIC2a chimeras showed that swapping the thumb domain between subunits results in faster channel desensitization. Likewise, the covalent modification of Cys residues at selected positions in the β-ball-thumb interface accelerates the desensitization of the mutant channels. Studies of accessibility with thiol-reactive reagents revealed that the β-ball and thumb domains reside apart in the resting state but that they become closer to each other in response to extracellular acidification. We propose that the thumb domain moves upon continuous exposure to an acidic extracellular milieu, assisting with the closing of the pore during channel desensitization.

Acid-sensing ion channels (ASICs)[2] are voltage-insensitive cation-permeable channels expressed in neurons of the peripheral and central nervous systems that respond to sudden changes in extracellular pH. Four genes that encode for six ASIC subunits and splice variants have been identified in mammals (ASIC1a, ASIC1b, ASIC2a, ASIC2b, ASIC3, and ASIC4) (1–10). In the central nervous system, disruption of ASIC1a expression causes a number of learning and memory-related phenotypes (11–14). Conversely, activation of ASIC1a has been linked to neurotoxicity in a mouse model of brain ischemia (15) and in neurodegenerative diseases such as multiple sclerosis (16), Huntington disease (17), Parkinson disease (18), and spinal cord injury (19). There is a substantial body of research that indicates that ASIC subunits participate in nociception in peripheral neurons (20–22) as well as in pain processing in the central nervous system (23–25). Therefore, ASICs represent novel therapeutic targets to treat pain as well as neurological diseases.

ASIC subunits assemble to form homo- and heterotrimers that display distinct proton sensitivities for activation and desensitization kinetics (26–29). Although the molecular determinants for channel activation have been extensively investigated, less is known about the mechanisms that promote channel desensitization in the continual presence of protons. ASIC subunits contain two membrane-spanning helices that form the pore of the channel and connect to cytoplasmic N- and C-terminal regions and to a large extracellular loop with defined domains termed the wrist, thumb, finger, β-ball, knuckle, and palm (see Fig. 1) (30). In the solved structure of chicken ASIC1 (cASIC1) at low pH, the β-ball and palm domains are packed in the interior of the assembled homotrimer, whereas the α-helical finger, thumb, and knuckle domains are distributed in the periphery of the ectodomain (see Fig. 1). The extracellular region is connected to the transmembrane helices by short loops in the wrist. Because of their location, solvent-accessible surface area, and presence of protonable residues, the finger, β-ball, and thumb domains have been considered part of the ASIC-sensing machinery (30). The importance of finger-thumb and β-ball-thumb movements to channel activation has been underscored by the solved structure of cASIC1 in complex with psalmotoxin (31, 32), a peptidic toxin derived from the venom of the tarantula *Psalmopoeus cambridgei* and with MitTx (33), a heterodimeric peptidic toxin isolated from the Texas coral snake (*Micrurus tener*) venom. Psalmotoxin and MitTx have modulatory effects on ASIC1a. Psalmotoxin desensitizes the channel at neutral pH (34) but yields steady-state currents at acid pH values (31). MitTx acts as a channel agonist that induces a slow activation at neutral pH (21). Interestingly, psalmotoxin forms non-polar interactions with residues in the thumb and polar interactions with acidic residues in the finger, β-ball, and thumb domains of one subunit and the palm domain of the neighboring subunit (31, 32). MitTX forms extensive interactions with residues in the thumb domain and wrist of cASIC1 subunits, locking the channels in a constitutively active state (33). On the whole, these findings support the notion that the finger, β-ball, and thumb domains are essential components of the gating machinery of the channel.

* This work was supported by National Institutes of Health Grants R01 DK084060, T32 DK061296, and by Cellular Physiology Core of the Pittsburgh Center for Kidney Research Grant P30-DK079307. The authors declare that they have no conflicts of interest with the contents of this article. The content is solely the responsibility of the authors and does not necessarily represent the official views of the National Institutes of Health.

[1] To whom correspondence should be addressed: Renal-Electrolyte Division, Dept. of Medicine, S935 Scaife Hall, 3550 Terrace St., Pittsburgh, PA 15261. Tel.: 412-648-9075; E-mail: mdc4@pitt.edu.

[2] The abbreviations used are: ASIC, acid-sensing ion channel; MTS, methanethiosulfonate; MTSMT, [1-(trimethylammonium)methyl] methanethiosulfonate; MTSET, [2-(Trimethylammonium)ethyl] methanethiosulfonate; MTSPT, [3-(trimethylammonium)propyl] methanethiosulfonate; CI, confidence interval; pH50, pH of half-maximal activation.

Given the importance of the thumb and neighboring domains to channel activation and desensitization, we examined their contribution to these processes through the analysis of ASIC1a-ASIC2a chimeras, by assessing the effect of covalent modification of introduced Cys at the finger-thumb and β-ball-thumb interfaces, and through studies of accessibility with thiol-reactive reagents in the resting and desensitized states. Our data indicate that the introduction of structural changes at the β-ball-thumb interface accelerates channel desensitization. Studies with thiol-reactive reagents showed a change in accessibility in the thumb domain when the channel transitions from the resting to the desensitized state. Based on these results, we propose that the thumb domain moves in response to extracellular acidification to contain the movements of the β-ball and palm domains. Our data indicate that the thumb domain plays an essential role in the process that shuts down ion conduction during desensitization.

Experimental Procedures

Molecular Biology and Oocyte Expression—Murine ASIC1a and ASIC2a were cloned in the pSP64 Poly(A) (Promega) and pcDNA3.1/Hygro (+) (Life Technologies) vectors, respectively. To generate ASIC1a-ASIC2a chimeras, double-stranded gBlock gene fragments (Integrated DNA Technologies) coding for the ASIC1a and ASIC2a finger and thumb domains were amplified by PCR using specific primers and cloned in the ASIC1a-pSP64 Poly(A) and ASIC2a-pcDNA3.1/Hygro (+) backbones using standard cloning techniques. The residues that were swapped between ASIC1a and ASIC2a to generate the finger-thumb chimeras are shown in Fig. 1*B*. Site-directed mutagenesis was performed using the QuikChange XL site-directed mutagenesis kit (Agilent Technologies). All constructs were confirmed by direct sequencing. cDNAs were transcribed with SP6 or T7 mMessage mMachine (Applied Biosystems) according to the instructions of the manufacturer. Oocytes in stages 5–6 were harvested from adult female *Xenopus laevis* (Nasco) in accordance with a protocol approved by the University of Pittsburgh Institutional Animal Care and Use Committee. Oocytes were injected with 0.05–6 ng of cRNA coding for ASIC wild-type and mutant channels and maintained at 18 °C in modified Barth's solution containing 88 mM NaCl, 1 mM KCl, 2.4 mM $NaHCO_3$, 15 mM HEPES, 0.3 mM $Ca(NO_3)_2$, 0.41 mM $CaCl_2$, 0.82 mM $MgSO_4$, 10 μg/ml sodium penicillin, 10 μg/ml streptomycin sulfate, and 100 μg/ml gentamycin sulfate (pH 7.4).

Two-electrode Voltage Clamp—Electrophysiological experiments were performed at room temperature 1–2 days after injection. Oocytes were placed in a chamber with a volume of ~20 μl (Automate Scientific) and continuously perfused by gravity at a rate of 8–10 ml/min with a solution containing 110 mM NaCl, 2 mM KCl, 1 mM $CaCl_2$, and 10 mM HEPES (pH 8.0). Acidic test solutions of pH 4.5–6.5 were buffered with MES, and test solutions of pH 3–4 were buffered with glycine. In anion substitution experiments, we replaced NaI or CH_3SO_3Na ($MeSO_3Na$) for NaCl. Two-electrode voltage clamp was performed with a TEV-200A amplifier (Dagan Corp.) as previously described (35). Data were captured with a Digidata 1440A acquisition system using pClamp 10 (Molecular Devices). Glass electrodes filled with 3 M KCl with resistances of 0.2–2 MΩ were employed to impale the oocytes. Oocytes were continuously clamped at −60 mV.

Modification of Cys Residues—1-(Trimethylammonium)methyl methanethiosulfonate (MTSMT), 2-(trimethylammonium)ethyl methanethiosulfonate (MTSET), and 3-(trimethylammonium) propyl methanethiosulfonate (MTSPT) were dissolved in recording buffer at a concentration of 1.0 mM. The half-time of hydrolysis of MTSET in the recording solution of pH 7.0 is 130 min (36). Therefore, solutions buffered at pH 7.0 containing MTS reagents were used within 30 min of preparation. Because MTS reagents are relatively unstable in alkaline solutions, MTSET in buffer of pH 8.0 was used immediately after preparation.

Data Analysis—Data are expressed as the mean ± S.E. (*n*), where *n* indicates the number of independent experiments analyzed. Parametric or nonparametric tests were employed as appropriate, and $p < 0.05$ was considered statistically significant. No mathematical correction was made for multiple comparisons with a *t* test. Assuming all null hypotheses are true, we expect 5% of the comparisons to have uncorrected *p* values of less than 0.05. The pH of half-maximal activation (pH_{50}) was calculated from normalized pH-evoked peak currents plotted as a function of the pH of activation. Data were fitted to a standard monotonic sigmoid dose-response curve. pH_{50} is expressed as the mean ± S.E. with a 95% confidence interval (CI). The time constant of macroscopic desensitization is defined as the current decay in the continual presence of agonist. To estimate the time constants of macroscopic desensitization, the decay phase of the pH-evoked response was fitted to a single exponential function with Clampfit (Molecular Devices). Fitting of dose-response relationships and statistical comparisons was performed with GraphPad 5.03 (GraphPad Software).

Results

The ASICs Thumb Domain Controls Desensitization—To assess the contribution of the finger and thumb domains to proton activation and desensitization, a series of chimeras were generated by swapping these domains between ASIC1a and ASIC2a. Structurally, the thumb domain is relatively well conserved between these two subunits, with 76.4% sequence identity, whereas the finger domain shows more variability with 58.6% sequence identity (Fig. 1*B*). We chose these ASIC subunits because the apparent proton affinity for activation of homomeric ASIC1a and ASIC2a channels differs by almost three pH units (Fig. 2*B*). In addition, ASIC2a desensitizes notably slower than ASIC1a (Fig. 2*C*). We produced five chimeras, ASIC1a with the finger domain of ASIC2a (ASIC1a-F2a), ASIC1a with the thumb domain of ASIC2a (ASIC1a-T2a), ASIC1a with the finger and thumb domains of ASIC2a (ASIC1a-FT2a), ASIC2a with the thumb domain of ASIC1a (ASIC2a-T1a), and ASIC2a with the finger and thumb domains of ASIC1a (ASIC2a-FT1a) (Fig. 2*A*). The estimated pH value of half-maximal activation (pH_{50}) for ASIC1a was 6.32 ± 0.07 (CI 6.18–6.48), for ASIC2a was 3.54 ± 0.04 (CI 3.47–3.62), for ASIC1a-F2a was 6.76 ± 0.05 (CI 6.66–6.86), for ASIC1a-T2a was 6.26 ± 0.06 (CI 6.13–6.39), for ASIC1a-FT2a was 5.23 ± 0.05 (CI 5.14–5.32), for ASIC2a-T1a was 3.60 ± 0.05 (CI 3.50–

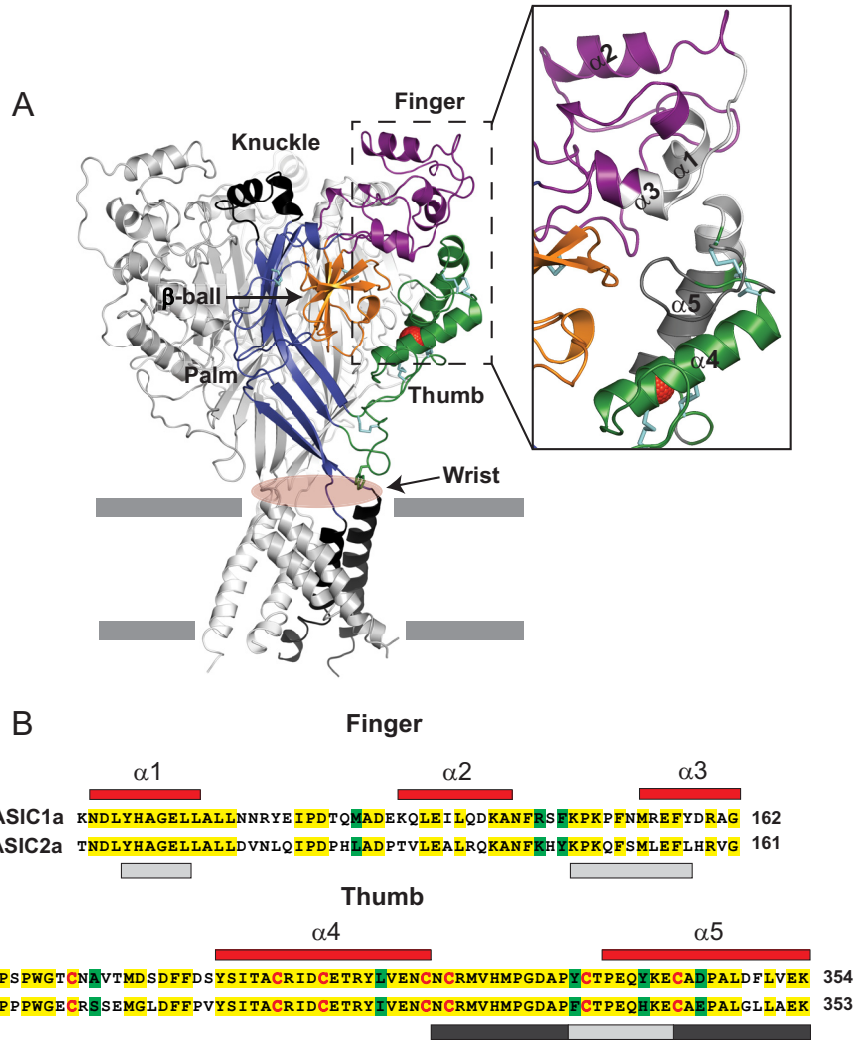

FIGURE 1. **Architecture of the finger and thumb domains.** *A*, schematic of cASIC1 in the desensitized state, illustrating the domain organization of each subunit (PDB code 4NYK). Disulfide bridges are shown as *cyan sticks*. The Cl^- ion bound to the thumb domain is shown in *red*. mASIC1a and cASIC1 share 89.6% amino acid identity. *Inset*, close-up view of the finger and thumb domains. The area within the finger and thumb domains examined in this work is shown in *gray*. Note that the *light gray region* in the finger domain (Tyr^{109}-Leu^{114} and Lys^{148}-Tyr^{158}) is in close proximity to the *light gray region* in the thumb domain (Tyr^{334}-Glu^{342}). The region highlighted in the thumb domain in *dark gray* is located near the β-ball domain in the desensitized state. *B*, sequence alignment of the mASIC1a and mASIC2a finger and thumb domains. mASIC1a numbered α helices (*red*) are shown above their corresponding amino acids. Identical residues are highlighted in *yellow*, whereas conserved residues are highlighted in *green*. Conserved cysteine residues are shown in *red*. The areas within the finger and thumb domains examined in Figs. 5 and 6 are shown in *light* and *dark gray* (see above).

3.69), and for ASIC2a-FT1a was 3.72 ± 0.04 (CI 3.65–3.79) (Fig. 2*B*). These results show that the individual substitution of the finger or thumb domain of ASIC2a into ASIC1a (ASIC1a-F2a and ASIC1a-T2a) does not alter the apparent proton affinity for activation. Although combined swapping of the finger and thumb domains of ASIC2a into ASIC1a (ASIC1a-FT2a) resulted in a shift in apparent proton affinity toward more acidic pH values, the swapping of ASIC1a finger and/or thumb domains into ASIC2a (ASIC2a-T1a and ASIC2a-FT1a) did not change the apparent proton affinity for activation. Together, these results suggest that the finger and thumb domains do not contain the structural components that determine the difference in proton sensitivity between ASIC1a and ASIC2a.

To evaluate the contribution of the finger and thumb domains to macroscopic desensitization, we compared the current decay upon continual exposure to protons of ASIC1a, ASIC2a, and chimeras. In Fig. 2*D*, we plotted the rates of desensitization of ASIC1a and ASIC2a as a function of the pH of activation. We compared the rates of desensitization of ASIC1a, ASIC1a-F2a, ASIC1a-T2a, and ASIC1a-TF2a at pH 5 (maximal activation) with the rates of ASIC2a at pH 4.0 (Fig. 2*E*). Note that ASIC2a, ASIC2a-T1a, and ASIC2a-FT1a do not respond to an acidification to pH 5.0. Because ASIC2a-T1a and ASIC2a-FT1a required a higher $[H^+]$ for maximal activation than channels with an ASIC1a backbone, the rates of desensitization of these chimeric channels were compared at pH 4 (Fig. 2*F*). Our data show that swapping the thumb domain of ASIC2a into ASIC1a accelerates channel desensitization (Fig. 2*E*). Likewise, swapping the thumb domains of ASIC1a into ASIC2a resulted in faster rates of channel desensitization, which occurs without any noticeable change in channel activation (Fig. 2*F*). Together, these results suggest that the thumb domain has an important role in ASIC desensitization.

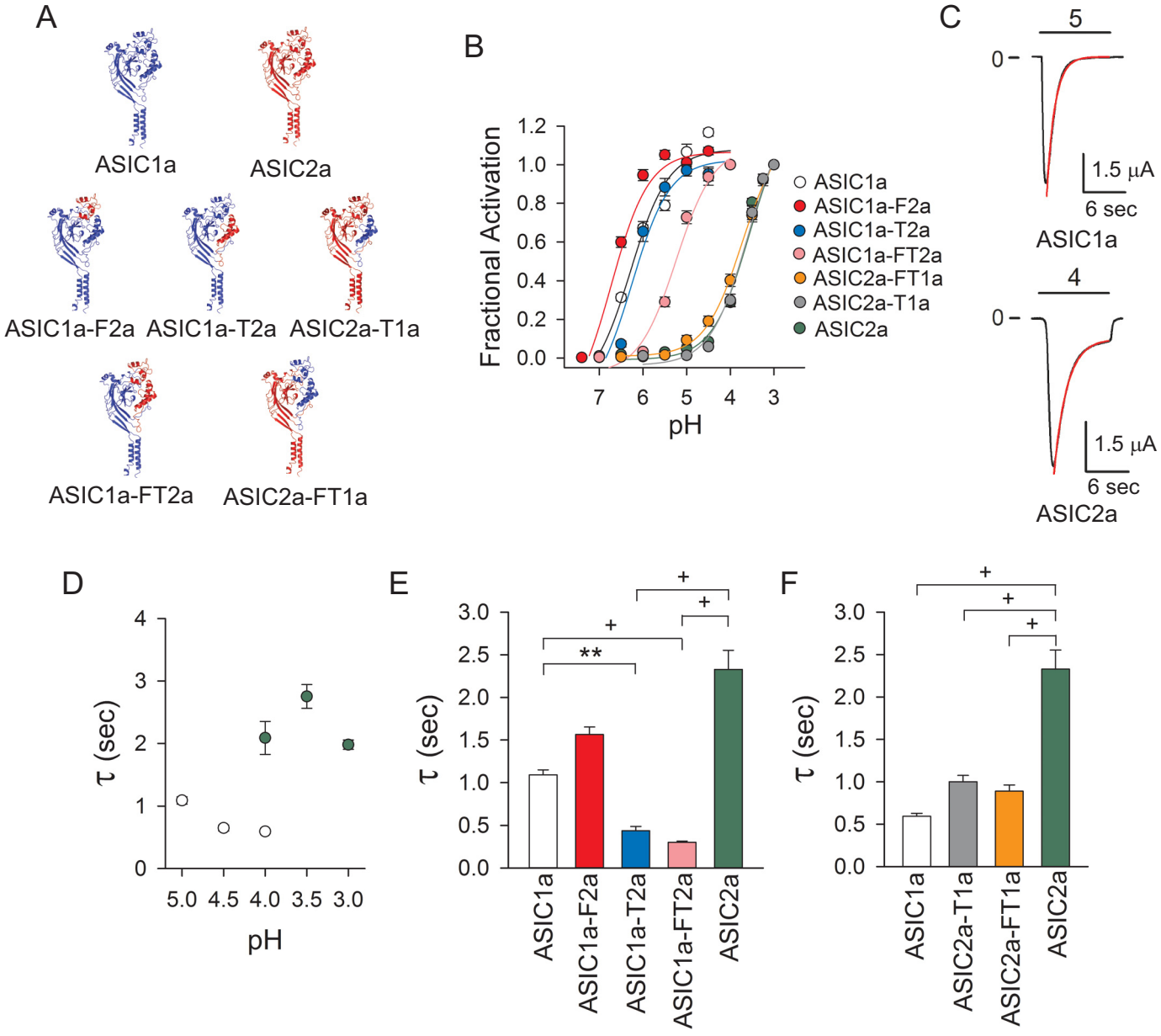

FIGURE 2. **Thumb domain interactions affect desensitization.** *A*, topological models for ASIC1a (*blue*), ASIC2a (*red*), ASIC1a-F2a, ASIC1a-T2a, ASIC1a-FT2a, ASIC2a-T1a, and ASIC2a-FT1a. Constructs were generated by swapping the finger and thumb domains between ASIC1a and ASIC2a (sequences in Fig. 1*B*). *B*, dose-response activation curves for ASIC1a, ASIC2a, and finger-thumb chimeras. Proton-activated currents were elicited by a drop in extracellular pH from 8.0 to solutions of lower pH. To determine statistical significance, the confidence intervals for the pH_{50} values of ASIC1a, ASIC2a, and finger-thumb chimeras were compared. Statistically significant differences in apparent proton affinity were found between ASIC2a, ASIC2a-T1a, ASIC2a-FT1a, ASIC1a-F2a, and ASIC1a-FT2a with ASIC1a and between ASIC1a, ASIC1a-F2a, ASIC1a-T2a, ASIC1a-FT2a, and ASIC2a-FT1a with ASIC2a ($n = 10–31$, $p < 0.05$). *C*, representative recordings of experiments conducted with oocytes expressing ASIC1a and ASIC2a. The whole-cell current decay after extracellular acidification was fitted to a single exponential function as described under "Experimental Procedures" (*red lines*). *D*, time constant (τ) of desensitization of ASIC1a and ASIC2a as a function of pH of activation ($n = 10–53$). *E* and *F*, time constants of desensitization of ASIC1a, ASIC2, and finger-thumb chimeras. Time constants of desensitization were determined as described above. *E*, the time constants of desensitization of ASIC1a, ASIC1a-F2a, ASIC1a-T2a, and ASIC1a-FT2a at pH 5.0 and of ASIC2 at pH 4.0 ($n = 13–46$). *F*, the time constants of desensitization of ASIC1a, ASIC2a-T1a, ASIC2a-FT1a, and ASIC2a at pH 4.0 ($n = 12–28$). Statistically significant differences in the time constants of desensitization between ASIC1a, ASIC2a, and chimeric channels are indicated. **, $p < 0.01$; +, $p < 0.001$ (analysis of variance followed by Dunn's multiple comparisons test).

ASIC activity is modulated by extracellular anions (37, 38). Remarkably, the solved structure of ASIC1a in the desensitized state revealed the presence of a Cl^- binding site formed by two residues (Arg^{309} and Glu^{313}) of the α4 helix of one subunit and a residue (Lys^{211}) in the β-ball of the neighboring subunit (30). Mutations at the Cl^- binding site of ASIC1a accelerate desensitization and dramatically reduce tachyphylaxis, suggesting that extracellular Cl^- stabilizes the open state of the channel (38). ASIC2a desensitization is only partially dependent on the intersubunit Cl^- binding site (37). To determine whether acceleration of desensitization by thumb transposing is due to disruption of the Cl^- binding site, we examined the effect of anion substitution on the response to extracellular acidification of ASIC1a, ASIC2a, and chimeras. Fig. 3*A* shows representative tracings of experiments conducted with oocytes expressing ASIC1a or ASIC2a in the presence of extracellular Cl^-,

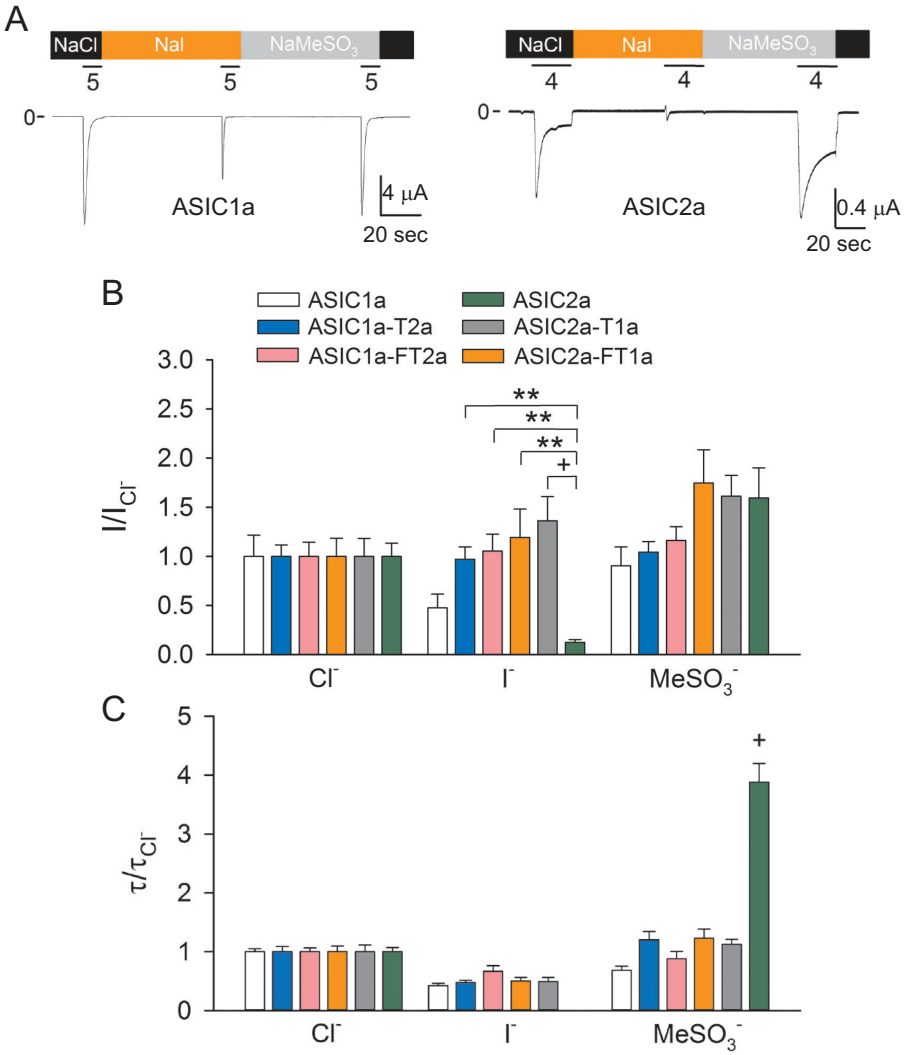

FIGURE 3. **Extracellular anion modulation of ASIC1a, ASIC2a, and finger-thumb chimeras.** *A*, representative recordings of experiments conducted with oocytes expressing ASIC1a and ASIC2a in solutions containing Cl^-, $MeSO_3^-$, or I^-. Whole-cell currents were elicited by a change in extracellular pH from 8.0 to 5.0 (ASIC1a) or 4.0 (ASIC2a). Note that ASIC2a does not response to extracellular acidification in the presence of I^-. *B*, effect of anion substitution on the response to extracellular acidification of ASIC1a, ASIC2a, and chimeras. Whole-cell currents were evoked by a change in extracellular pH from 8.0 to 5.0 (ASIC1a, ASIC1a-F2a, ASIC1a-T2a, and ASIC1a-FT2a) or to 4.0 (ASIC2a, ASIC2a-T1a, and ASIC2a-FT1a). The relative response ($I/I_{Cl}-$) represents the ratio of the pH-elicited peak current to the pH-elicited peak current in Cl^-. **, $p < 0.01$; +, $p < 0.001$ ($n = 10–14$) (Kruskal-Wallis test followed by Dunn's multiple comparisons test). *C*, effect of anion substitution on the time constants of desensitization of ASIC1a, ASIC2a, and chimeras. The time constants of desensitization were estimated by fitting the current decay after extracellular acidification to a single exponential function as described under "Experimental Procedures." For ASIC1a, ASIC1a-F2a, ASIC1a-T2a, and ASIC1a-FT2a, currents were evoked by a drop in extracellular pH from 8.0 to 5.0, whereas for ASIC2a, ASIC2a-T1a, and ASIC2a-FT1a, currents were elicited by a drop in extracellular pH from 8.0 to 4.0. Statistically significant difference with ASIC1a and chimeras is indicated. +, $p < 0.001$ ($n = 10–14$) (analysis of variance followed by Tukey's multiple comparisons test).

$MeSO_3^-$, and I^-. As described previously by Kusama *et al.* (37, 38), $MeSO_3^-$ and I^- accelerated the desensitization of ASIC1a (Fig. 3*A*, *left panel*). $MeSO_3^-$ dramatically slows down the desensitization of ASIC2a, whereas I^- completely blocked the response to extracellular acidification (Fig. 3*A*, *right panel*). To compare the effect of anion substitution among wild-type and chimeric channels, the response to extracellular acidification and rate of desensitization obtained in Cl^-, $MeSO_3^-$, and I^- was normalized to the response attained with a solution containing Cl^-. We found that anion substitution causes similar changes in the rate of desensitization and magnitude of the response to extracellular acidification of ASIC1a-T2a, ASIC1a-FT2a, ASIC2a-T1a, ASIC2a-FT1a, and ASIC1a (Fig. 3, *B* and *C*). Notably, none of the chimeras resembled the response of ASIC2a to extracellular anions. These findings indicate that transposing the thumb of ASIC2a into ASIC1a does not alter anion selectivity, consistent with the notion that acceleration of desensitization is not due to the disruption of the anion site in ASIC1a.

Chemical Modification of Residues at the Finger-Thumb and β-Ball-Thumb Interfaces Alters Channel Activation and Desensitization—To further examine functional interactions between the thumb and neighboring domains in ASIC1a, we employed the substituted cysteine accessibility method (39). Cys substitutions were introduced in the finger domain in the tracts spanning from Tyr^{109} to Leu^{114} and from Lys^{148} to Tyr^{158} and in the thumb domain in the tract spanning from Asp^{322} to Lys^{354}. Note that residues in tract 334–342 of the thumb domain reside in close proximity to the finger (Fig. 1*A*, *light gray*). Residues in tracts 322–333 and 344–354 of the thumb

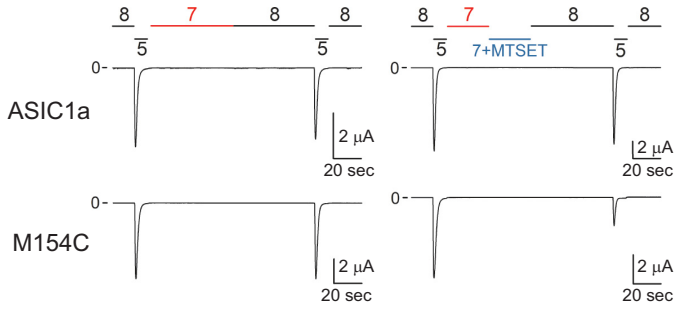

FIGURE 4. **Chemical modification of M154C channels by MTSET.** Shown are representative recordings of experiments conducted with oocytes expressing control (C70L) and M154C mutant channels. Whole-cell currents were elicited by a change in extracellular pH from 8.0 to 5.0 before and after MTSET treatment. Oocytes expressing control and mutant channels were exposed to MTSET (1 mM) at pH 7.0, *i.e.* channels in the desensitized state (*right tracings*). Non-treated oocytes served as controls (*left tracings*).

domain reside near the β-ball domain in the desensitized state (Fig. 1*A*, *dark gray*). ASIC1a resides in a resting proton-sensitive state at pH 8.0 and in a desensitized proton-insensitive state at pH 7.0 (40). Because the majority of the residues in the finger and thumb domains are predicted to be solvent-accessible in the desensitized state using Swiss PDB viewer (41), we treated channels bearing Cys substitutions in these domains with MTSET at pH 7.0. MTSET is a bulky reagent with a trimethylammonium group that reacts with accessible unpaired Cys residues. Channels bearing Cys substitutions and controls were activated by a drop in extracellular pH from 8.0 to 5.0 before and after MTSET (1 mM) treatment at pH 7.0 (see representative tracings in Fig. 4). The relative response to extracellular acidification, which represents the ratio of the peak current evoked by extracellular acidification after MTSET treatment relative to the peak current evoked by extracellular acidification before treatment, was used to quantify the impact of MTSET treatment on ASIC1a activation (Fig. 5). Oocytes expressing mASIC1a bearing a Cys-to-Leu mutation at position 70 (C70L) served as controls for these experiments. We identified four positions in the finger domain (111, 113, 152, and 154) and 12 positions in the thumb domain of ASIC1a (325, 326, 327, 338, 339, 340, 344, 345, 347, 348, 351, and 352) where MTSET treatment altered the response to extracellular acidification (Fig. 5, *A* and *B*). Residues at positions 338, 339, and 340 in the thumb domain reside in close proximity to residues at positions 111, 113, 152, and 154 in the finger domain (Fig. 5*C*). Residues at positions 325, 326, 327, 344, 345, 347, 348, 351, and 352 in the thumb domain point toward residues in the β-ball domain in the solved structure of cASIC1 in the desensitized state (Fig. 5*C*). Helical wheel representation of the thumb domain α5 situates residues Tyr^{340}, Ala^{344}, Asp^{345}, Ala^{347}, Leu^{348}, Leu^{351}, and Val^{352} on the same side of the helix, facing residues in the β-ball domain (data not shown). Overall, these results show that the chemical modification of Cys residues at selected positions in the finger-thumb and β-ball-thumb interfaces alters the response to extracellular acidification.

To examine the consequences of structural modifications at the finger-thumb and β-ball-thumb interfaces on ASIC1a desensitization, we measured the rates of macroscopic desensitization for channels bearing single Cys mutations in the finger domain in the tracts spanning from Tyr^{109} to Leu^{114} and from Lys^{148} to Tyr^{158} and in the thumb domain in the tract spanning from Asp^{322} to Lys^{354}. Although individual Cys substitutions in the finger domain did not alter the rates of desensitization of ASIC1a, significant changes were apparent on channels bearing Cys mutations in the thumb domain at positions 327, 339, 346, 348, 350, and 351 (Fig. 6, *red symbols*). Furthermore, MTSET treatment accelerated the desensitization of channels bearing Cys mutations at positions 112, 154, 325, 326, 340, 345, 348, 351, and 352 (Fig. 6, *A* and *B*). Significantly, the helical wheel diagram situates the residues sensitive to MTSET treatment on the side of α5 helix interfacing with the β-ball domain (Fig. 6*C*). These data indicate that the introduction of structural changes at the β-ball-thumb interface accelerate channel desensitization.

Molecular Mechanism of Desensitization—ASIC activation encompasses the functional coupling of proton binding to sites in the extracellular region to pore opening, whereas desensitization involves the constriction of the pore upon continuous exposure to an acidic extracellular environment. Of note, ASIC1a desensitization does not require the transition of the channel through the open state because the exposure of ASIC1a to pH 7.2–7.0, which does not trigger activation, is sufficient to make it insensitive to extracellular protons (35). Our data indicate that the introduction of structural changes primarily at the β-ball-thumb interface influences channel activation as well as desensitization. Mechanistically, the magnitude of the response to extracellular acidification depends to some extent on the rate of channel desensitization. For instance, if the covalent modification of a particular mutant alters channel desensitization so that the rate of desensitization is fast enough to overwhelm the rate of activation, then the magnitude of the response to extracellular acidification after covalent modification will be diminished. To determine whether the observed drop in the magnitude of the response to extracellular acidification of Cys mutants treated with MTSET results from an increase in the rate of desensitization, we plotted the relationship between the relative response and the relative rate of desensitization for channels bearing a Cys mutation in the α5 helix (positions 337–354) (Fig. 7). The relative rate of desensitization represents the ratio of the desensitization rate after MTSET treatment to the desensitization rate before treatment. Correlation analysis of this set of data revealed that the magnitude of the response to extracellular protons shows a strong dependence on desensitization for channels bearing a Cys substitution in α5 (Fig. 7). This finding supports the notion that accelerated desensitization contributes to the observed drop in the response to extracellular acidification of the Cys mutants treated with MTSET.

To further investigate whether accelerated desensitization accounts for the observed changes in channel activation, we generated proton dose-response curves for activation before and after MTSET treatment for F152C, M154C, M325C, and D345C mutants (Fig. 8, *A–D*). We selected these mutants because they are located at the interface between the β-ball, finger, and thumb domains (Fig. 5*C*). The covalent modification of D345C channels by MTSET shifted the dose-response curve toward more acidic pH values, from 6.11 ± 0.06 (CI 6.00–6.23) to 4.91 ± 0.06 (CI 4.80–5.02) (Fig. 8*D*). Similarly, the modification of M154C channels by MTSET shifted the pH_{50}

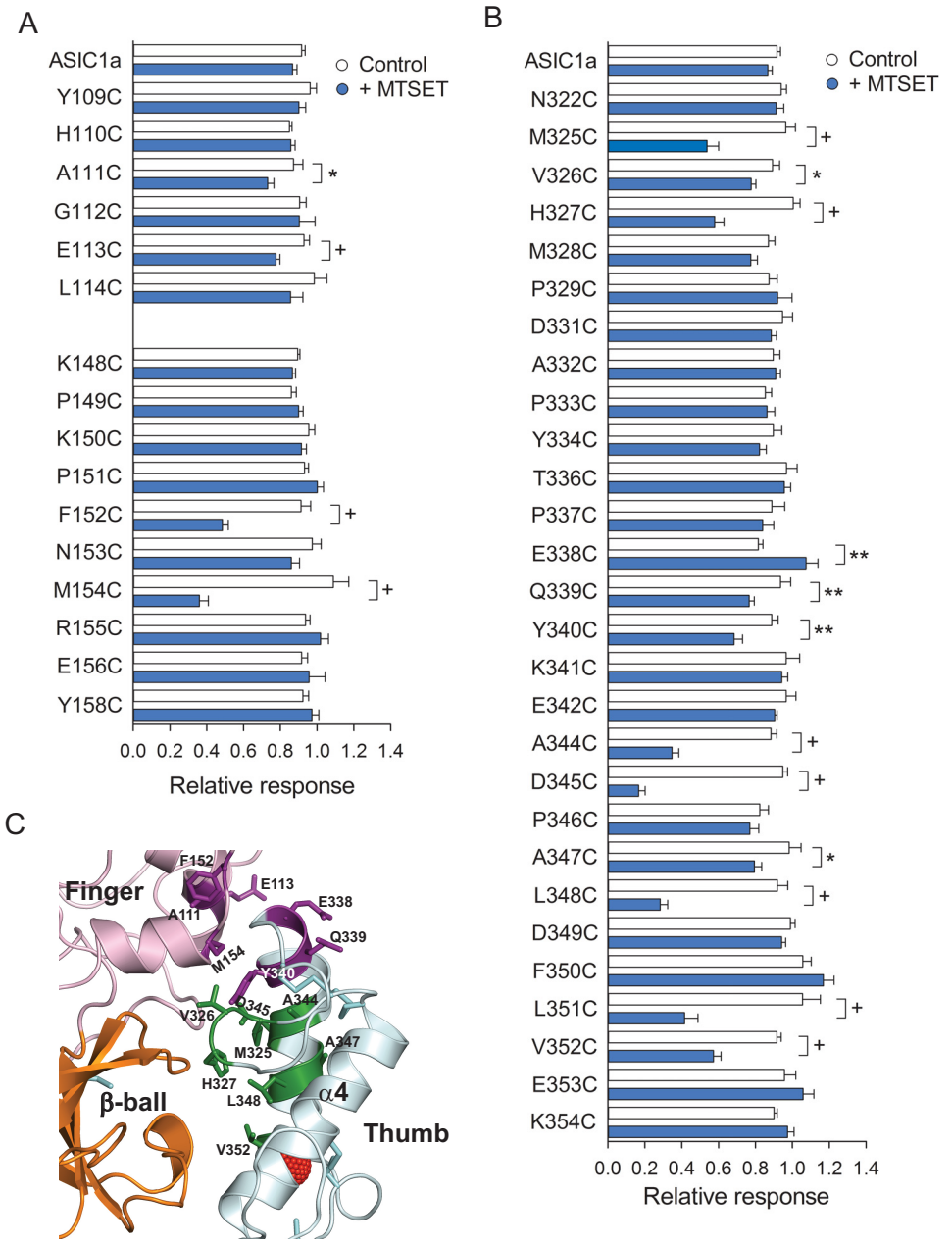

FIGURE 5. **Covalent modification of Cys residues at the finger-thumb and β-ball-thumb interfaces diminishes the response to extracellular acidification.** *A* and *B*, reactivity toward MTSET of channels bearing Cys substitutions at selected sites in the finger (*A*) and thumb (*B*) domains. Whole-cell currents were evoked by a change in extracellular pH from 8.0 to 5.0 before and after MTSET treatment. The relative response represents the ratio of the pH-elicited peak current following MTSET treatment (or control) to the pH-elicited peak current before treatment. *, $p < 0.05$; **, $p < 0.01$; +, $p < 0.001$ ($n = 9$–36) (*t* test). *C*, schematic illustrating sites in the finger and thumb domains sensitive to MTSET treatment when mutated to Cys. Disulfide bridges are shown as *cyan sticks*. Sensitive sites in the finger domain are colored *purple*. Sensitive sites in the thumb domain colored *purple* (Glu^{338}, Gln^{339}, and Tyr^{340}) reside near the finger domain, whereas sites colored *green* (Met^{325}, Val^{326}, His^{327}, Ala^{344}, Asp^{345}, Ala^{347}, Leu^{348}, Leu^{351}, and Val^{352}) reside near the β-ball domain.

values from 6.06 ± 0.06 (CI 5.95–6.18) to 5.24 ± 0.07 (CI 5.11–6.37) (Fig. 8*B*). These results indicate that, for the M154C and D345C mutants, the observed changes in the magnitude of the response after MTSET treatment result from a shift in apparent proton affinity. This is consistent with our previous studies showing that the chemical modification of D345C channels by MTSET shifts the apparent proton affinity (42). In contrast, the covalent modification of F152C and M325C channels did not alter proton dose-response activation curves (Fig. 8, *A* and *C*). The last result is consistent with the notion that the covalent modification by MTSET of Cys residues at positions 152 and 325 impacts the molecular mechanisms that govern channel desensitization. To further substantiate this finding, we conducted additional experiments with thiol-reactive reagents of different lengths on channels bearing Cys mutations at positions 152, 154, 325, and 345. Fig. 8, *E–L* displays the relative response to extracellular acidification and the rates of desensitization for F152C, M154C, M325C, and D345C channels before and after treatment with MTSMT, MTSET, and MTSPT. Notably, for the most part, the effect of MTS treatment on these mutant channels was independent of the length of the transferable moiety of the thiol-reactive reagent. In gen-

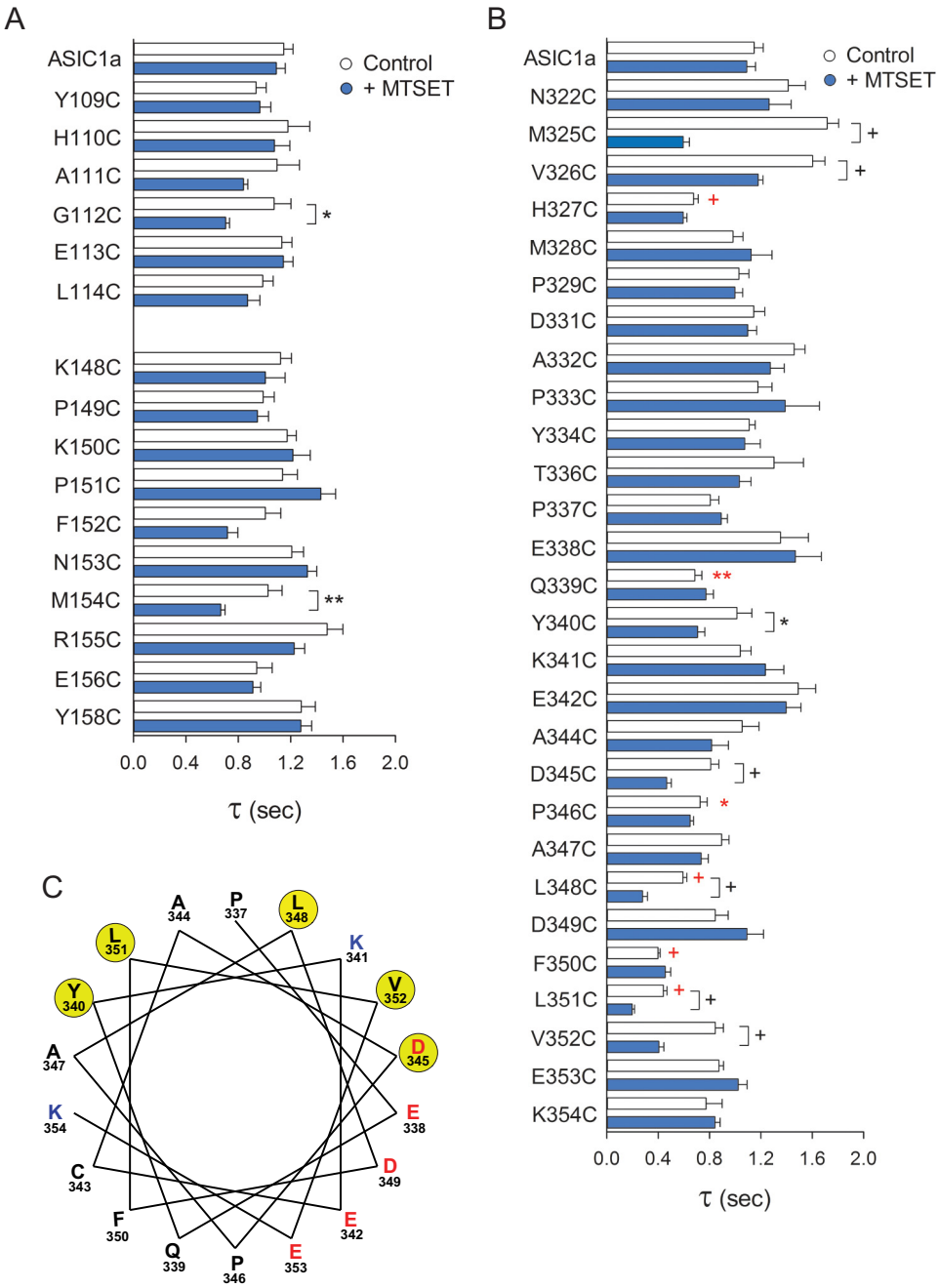

FIGURE 6. **Attachment of moieties at selected sites in the finger-thumb and β-ball-thumb interfaces accelerates desensitization.** *A* and *B*, effect of MTSET treatment on the rates of desensitization of channels bearing Cys substitutions in the finger (*A*) and thumb (*B*) domains. Whole-cell currents were evoked by a change in extracellular pH from 8.0 to 5.0 before and after MTSET treatment. The time constants of desensitization were estimated by fitting the current decay after extracellular acidification from 8.0 to 5.0 to a single exponential function as described under "Experimental Procedures." Statistically significant differences with the untreated control are indicated. *, $p < 0.05$; **, $p < 0.01$; +, $p < 0.001$ ($n = 9–36$) (*t* test). Statistically significant differences in the time constant of desensitization between untreated mutant channels and controls (ASIC1a C70L) are indicated in *red* (Kruskal-Wallis test followed by Dunn's multiple comparisons test). *C*, Helical wheel representation of positions in the α5 helix where the introduction of Cys mutation and MTSET treatment alter the rates of desensitization (*yellow*). Negatively charged and positively charged amino acids are notated in *red* and *blue*, respectively.

eral, the attachment of transferable moieties at positions 152, 154, 325, and 345 reduced the magnitude of the response to extracellular acidification and accelerated desensitization. Overall, these results expose two mechanisms by which the attachment of moieties alters the response to extracellular acidification: by changing apparent proton affinity and by increasing the rate of desensitization.

The Thumb Domain Moves during Desensitization—To gain an understanding of the underlying process that governs desensitization, we examined the accessibility of the Cys residue at position 344 toward MTSET in the resting and desensitized states (Fig. 9). We selected this residue because is located in the region of the α5 helix where the introduction of structural changes alters channel desensitization. For these experiments, currents were evoked on oocytes expressing A344C channels by a drop in extracellular pH from 8.0 to 5.0 before and after treatment with MTSET for 10, 30, 60, or 120 s. Oocytes were exposed to MTSET at pH 7.0 (*i.e.* channels residing in the

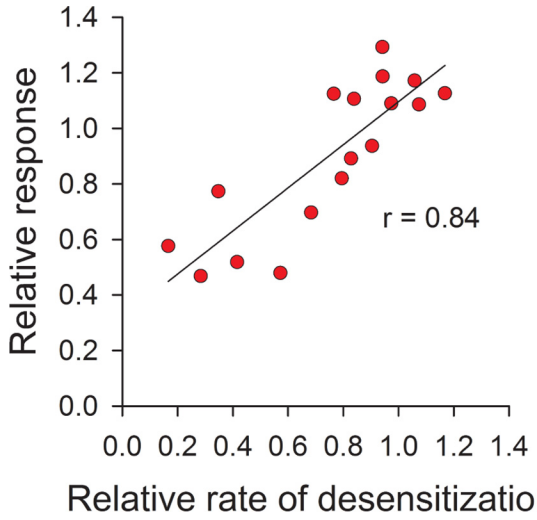

FIGURE 7. **Correlation analysis of the effect of covalent modification on the activation and desensitization of channels bearing Cys mutations in α5.** The mean value for the relative response and relative rate of desensitization after MTSET treatment of individual mutants in the tract P337C to K354C are plotted. The relative response for each mutant represents the mean of the ratio of the pH-elicited peak current following MTSET treatment to the mean of the pH-elicited peak current before treatment (data from Fig. 5). The relative rate of desensitization for each mutant represents the mean of the desensitization rate following MTSET treatment to the mean of the desensitization rate before treatment (data from Fig. 6). Data were analyzed using Pearson's correlation test ($r = 0.84$).

desensitized state) or at pH 8.0 (*i.e.* channels residing in a resting state) (Fig. 9*A*). Note that ASIC1a responds to extracellular acidification from a preconditioning pH of 8.0 (resting state) but not from a preconditioning pH of 7.0 (desensitized state). Proton-evoked currents after MTSET treatment were normalized to the current elicited by extracellular acidification before treatment. Fig. 9*B* shows the relative response to extracellular acidification for A344C channels as a function of the time of exposure to MTSET at pH 7.0 (*open circles*) or pH 8.0 (*blue circles*). The time constant of modification by MTSET (1 mM) of A344C channels was 39.9 s (CI 32.5–51.6) at pH 7.0 and 23.9 s (CI 20.5–28.8) at pH 8.0. The observed changes in MTSET accessibility indicate that extracellular acidification drives a reorganization of the thumb domain. Based on the solved structure of cASIC1 in the desensitized state, these results are consistent with the displacement of the thumb domain toward the β-ball domains when the channel transitions from the resting to the desensitized state.

Discussion

Structural studies have provided great detail of the organization of cASIC1 in the desensitized state, the psalmotoxin-bound (low-pH) and nonselective (high-pH) states, and the MitTx-bound open state (30–33, 43). Although these studies presented snapshots of the structure of the channel in several functional states, they provide limited information regarding the molecular movements that occur in the extracellular region after proton binding that lead to pore opening and, later, to desensitization. In this study, we employed a combined approach to define the role of the finger, β-ball, and thumb domains in the activation and desensitization of ASICs.

Role of the Finger and Thumb Domains in Activation—Jasti *et al.* (30) initially proposed that a cluster of adjacent acidic residues between the β-ball, thumb, and palm domains of cASIC1 served as proton-coordination sites. We have shown that the neutralization of the acidic residues in this pocket (Glu^{219}, Asp^{237}, Glu^{238}, Asp^{345}, Asp^{349}, and Asp^{407}) does not alter the apparent proton affinity (42), which denotes that these residues are not part of the proton-sensing machinery. However, our work (42) and the work of others (44, 45) showed that non-conservative mutations in this region of the protein alter the apparent proton affinity, consistent with the notion that the introduction of structural changes at the β-ball-thumb interface impacts a nearby proton coordination site. In addition to the mentioned region, we identified a proton coordination site in the lower palm domain of ASIC1a formed by residues Glu^{79} and Glu^{416} (46). Remarkably, the neutralization of Glu^{79} or Glu^{416} in the palm domain or the insertion of bulky changes at selected positions in the β-ball-thumb interface result in biphasic proton activation curves (42). Channels bearing substitutions that impact the proton coordination sites in the palm and β-ball-thumb interface (E79K-E345K) required pHs lower than 3.0 for activation, significantly below the pH_{50} of activation of wild-type ASIC1a (6.32 ± 0.07). In this study, we found that the apparent proton affinity of ASIC1a-FT2a channels was significantly lower than the that of wild-type ASIC1a channels or ASIC1a channels carrying individual domains of ASIC2a (ASIC1a-F2a and ASIC1a-T2a). In addition, our studies with thiol-reactive reagents show that the introduction of moieties at selected positions in the finger-thumb and β-ball-thumb interfaces shift the apparent proton affinity toward more acidic values. This finding is in good agreement with our previous findings, which showed that the modification of selected sites at the β-ball-thumb interface interferes with the molecular mechanisms that drive pore opening in response to extracellular acidification (42). Notably, the exchange of the finger and thumb domains of ASIC2a by those from ASIC1a (ASIC2a-FT1a) did not alter the apparent proton affinity for activation, indicating that the finger and thumb domains do not contain the structural features that determine the difference in apparent proton affinity among these isoforms. We propose that the modifications at the finger and thumb domain interfaces hinder molecular rearrangements associated with activation in the core of the protein.

The Thumb Domain Is Part of the Desensitization Machinery—Despite the high amino acid sequence conservation, ASIC1a and ASIC2a exhibit marked differences in proton sensitivity for activation and in desensitization. Chimeric channels made by swapping the finger and thumb domains between ASIC1a and ASIC2a provide important insights into the mechanism that controls channel desensitization. Our studies showed that swapping the thumb domain between isoforms (ASIC1a-T2a, ASIC1a-FT2a, ASIC2a-T1a, and ASIC2a-FT1a) resulted in accelerated desensitization. Likewise, the modification by MTSET of Cys residues introduced at positions neighboring the β-ball domain (325, 326, 345, 348, 351, and 352) resulted in faster channel desensitization. Moreover, we identified several positions in the thumb domain where Cys substitutions *per se* resulted in significantly faster desensitization rates. Taken as a whole, our results suggest that the introduction of changes at the β-ball-thumb interface enables more effective closing of the channel pore upon extracellular acidification.

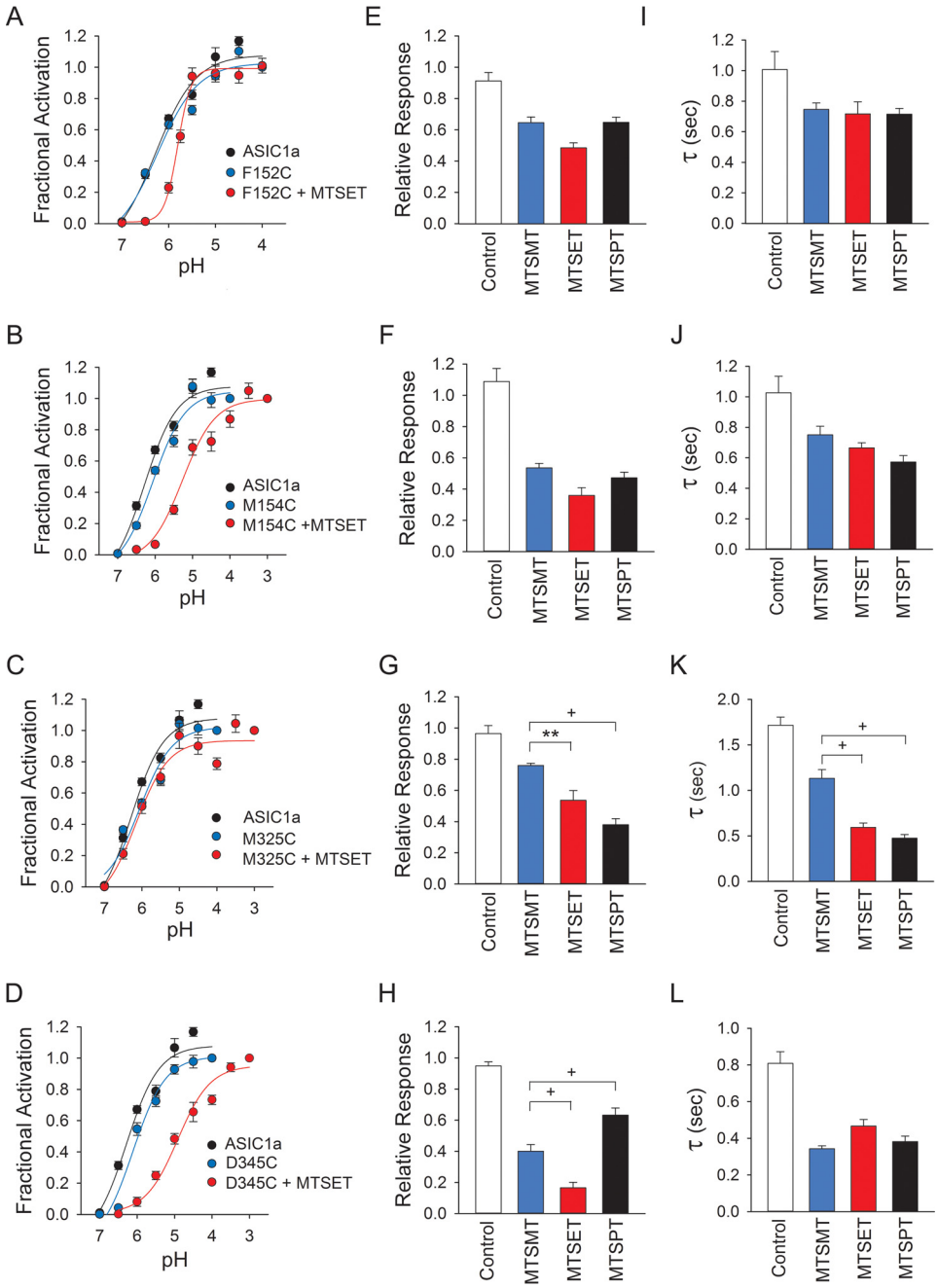

FIGURE 8. **Covalent modification of residues in the finger and thumb domains accelerates channel desensitization.** *A–D*, dose-response proton activation curves for channels bearing Cys mutations at selected positions in the finger and thumb domains. Proton-activated currents were elicited by a drop in extracellular pH from 8.0 to solutions of lower pH. To determine statistical significance, the confidence intervals for the pH_{50} values were compared. Statistically significant differences in apparent proton affinity between untreated and MTSET-treated channels were found for the M154C and D345C mutants ($n = 9–32$, $p < 0.05$). *E–H*, reactivity of F152C, M154C, M325C, and D345C channels toward thiol-reactive reagents of increasing length. Whole-cell currents were evoked by a change in extracellular pH from 8.0 to 5.0 before and after treatment with MTSMT, MTSET, or MTSPT at pH 7.0. Non-treated oocytes expressing mutant channels served as controls. Statistically significant differences are indicated. **, $p < 0.01$; +, $p < 0.001$ ($n = 10–14$, analysis of variance followed by Tukey's multiple comparisons test). *I–L*, time constants of desensitization for channels bearing Cys mutations at positions 152, 154, 325, and 345 before and after covalent modification with thiol-reactive reagents. +, $p < 0.001$ ($n = 10–14$, analysis of variance followed by Tukey's multiple comparisons test).

Kusama *et al.* (38) demonstrated that the substitution of extracellular Cl^- with methanesulfonate or the mutation of residues involved in Cl^- binding in the thumb or β-ball domains of ASIC1a accelerates desensitization without affecting pH dose responses for activation. Our anion substitution studies indicate that the acceleration of desensitization observed with the chimeras is not due to the disruption of the anion site in ASIC1a (Fig. 3) because ASIC1a, ASIC1a-T2a, and ASIC1a-FT2a displayed similar anion modulation. Indeed, swapping the thumb of ASIC2a into ASIC1a does not change the residues that form the Cl^- coordination site (Fig. 1*B*). Remarkably, ASIC2a anion modulation is only partially dependent on the Cl^- binding site at the thumb and β-ball domains (37). Our studies indicate that transposition of the thumb domain of ASIC1a into ASIC2a is sufficient to change its anion selectivity. This finding suggests that ASIC2a contains an additional anion coordination site with a

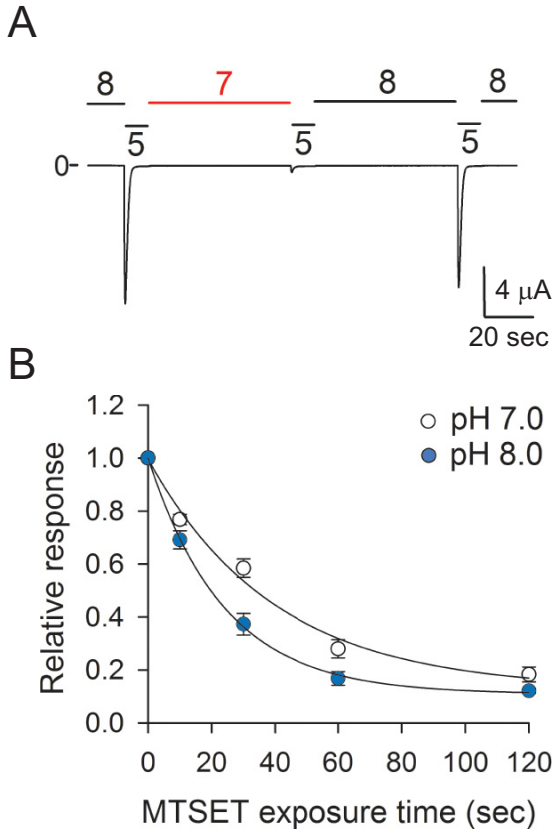

FIGURE 9. **State-dependent changes in accessibility in the thumb domain.** *A*, pH dependence of A344C channel desensitization. Whole-cell currents were elicited in oocytes expressing A344C channels by extracellular acidification from solutions of pH 7.0 or 8.0 to a solution of pH 5.0 ($n = 5$). Note that A344C channels reside in the desensitized state at pH 7.0 because they do not respond to extracellular acidification. *B*, chemical modification by MTSET of A344C channels in the resting and desensitized states. Whole-cell currents were elicited by a change in extracellular pH from 8.0 to 5.0 before and after treatment with MTSET reagents for 15, 30, 60, or 120 s. MTSET was applied at pH 7.0 (*open circles*), *i.e.* channels in the desensitized state, or at pH 8.0 (*blue circles*), *i.e.* channels in the resting state. The peak current elicited by extracellular acidification after MTSET treatment was normalized to the peak current elicited by extracellular acidification before treatment. To determine statistical significance, the confidence intervals for the time constants of modification were compared. The time constants of modification at pH 7.0 (mean 39.9, CI 32.5–51.6) and pH 8.0 (mean 23.9, CI 20.4–28.8) were statistically different ($p < 0.05$, $n = 13–33$).

dominant effect on channel desensitization and that swapping of the thumb domain disrupts this anion coordination site.

Mechanism of ASICs Desensitization—The desensitization of Cys loop receptors involves rearrangements of the M2/M3 interface, which mediates the constriction of the pore and consequent reduction of ion conductance (47–51). We propose that ASIC desensitization entails a series of conformational rearrangements that extend from the extracellular region to the pore of the channel. We and others reported state-dependent changes in accessibility to thiol-reactive reagents for sites in the upper pore (G428C), wrist (Y424C), and lower palm (E79C and E416C) domains of ASIC1a (35, 36, 46, 52–55). For instance, Cys residues introduced at positions 79 and 416 were covalently modified by MTSET at pH 8.0 but not at pH 7.0 (46), suggesting that the lower palm domain resides in an expanded conformation in the resting state and that it contracts upon extracellular acidification. Notably, the covalent modification of E79C channels by MTSET extended the time course of desensitization and impeded the complete closure of the pore upon continual exposure to an acidic environment (46). Likewise, mutation of selected residues in the palm domain of ASIC1a impairs desensitization by preventing the closing movement of the palm (55). A similar effect was observed with the covalent modification of G428C channels by MTSET (36). These results support the notion that the contraction of the lower palm domain and outer pore is required for pore closing during desensitization.

We posit that the thumb domain acts as a restrainer that prevents the movement of the lower palm and pore upon continual exposure to an acidic environment. Our findings indicate that the thumb domain does not initiate desensitization. If desensitization was determined by the β-ball-thumb domain interactions, then, by exchanging these domains among ASIC1a and ASIC2a, we should reverse the desensitization phenotype. However, we did not observe a reversion of the phenotype with the ASIC1a-ASIC2a chimeras, which suggests that the movements in the thumb domain are driven or occur in response to rearrangements in other parts of the protein. Our findings indicate that the introduction of structural changes in the thumb domain at positions bordering the β-ball domain accelerate the desensitization of the channel (Fig. 6). We postulate that the attachment of transferable moieties at the thumb domain facilitates physical interactions with neighboring domains, particularly the β-ball, assisting with the closing of the pore upon continuous exposure to an acidic milieu. The observed state-dependent changes in MTSET accessibility on A344C channels indicate that, in the resting state, the β-ball and thumb domains reside apart, but they become closer in response to extracellular acidification. This finding is consistent with voltage clamp fluorometry and luminescence resonance energy transfer studies, which reported a conformational reorganization of the thumb domain of ASIC1a in response to extracellular acidification (45, 56). The contribution of the finger domain to desensitization is less clear because we did not observe large changes in the time course of desensitization on channels bearing Cys mutations in the finger domain before or after MTSET treatment.

In summary, this study provides new insights into the molecular mechanism that governs ASICs desensitization. Our study shows that the covalent modification of sites primarily at the contact region between the β-ball and thumb domains results in accelerated desensitization and a drop in the magnitude of the response to extracellular acidification. This region could serve as potential drug target to treat neurological disorders caused by the activation of ASICs.

Author Contributions—A. J. K. generated the constructs, performed and analyzed the experiments, and contributed to the preparation of the figures and manuscript. M. D. C. conceived the study, designed the chimeras, performed the experiments, analyzed the data, prepared the figures, and wrote the manuscript. Both authors approved the final version of the manuscript.

References

1. Akopian, A. N., Chen, C. C., Ding, Y., Cesare, P., and Wood, J. N. (2000) A new member of the acid-sensing ion channel family. *Neuroreport* **11,**

2217–2222
2. Babinski, K., Lê, K. T., and Séguéla, P. (1999) Molecular cloning and regional distribution of a human proton receptor subunit with biphasic functional properties. *J. Neurochem.* **72,** 51–57
3. Bässler, E. L., Ngo-Anh, T. J., Geisler, H. S., Ruppersberg, J. P., and Gründer, S. (2001) Molecular and functional characterization of acid-sensing ion channel (ASIC) 1b. *J. Biol. Chem.* **276,** 33782–33787
4. Chen, C. C., England, S., Akopian, A. N., and Wood, J. N. (1998) A sensory neuron-specific, proton-gated ion channel. *Proc. Natl. Acad. Sci. U.S.A.* **95,** 10240–10245
5. de Weille, J. R., Bassilana, F., Lazdunski, M., and Waldmann, R. (1998) Identification, functional expression and chromosomal localisation of a sustained human proton-gated cation channel. *FEBS Lett.* **433,** 257–260
6. García-Añoveros, J., Derfler, B., Neville-Golden, J., Hyman, B. T., and Corey, D. P. (1997) BNaC1 and BNaC2 constitute a new family of human neuronal sodium channels related to degenerins and epithelial sodium channels. *Proc. Natl. Acad. Sci. U.S.A.* **94,** 1459–1464
7. Gründer, S., Geissler, H. S., Bässler, E. L., and Ruppersberg, J. P. (2000) A new member of acid-sensing ion channels from pituitary gland. *Neuroreport* **11,** 1607–1611
8. Lingueglia, E., Champigny, G., Lazdunski, M., and Barbry, P. (1995) Cloning of the amiloride-sensitive FMRFamide peptide-gated sodium channel. *Nature* **378,** 730–733
9. Price, M. P., Snyder, P. M., and Welsh, M. J. (1996) Cloning and expression of a novel human brain Na^+ channel. *J. Biol. Chem.* **271,** 7879–7882
10. Waldmann, R., Champigny, G., Voilley, N., Lauritzen, I., and Lazdunski, M. (1996) The mammalian degenerin MDEG, an amiloride-sensitive cation channel activated by mutations causing neurodegeneration in *Caenorhabditis elegans*. *J. Biol. Chem.* **271,** 10433–10436
11. Wemmie, J. A., Chen, J., Askwith, C. C., Hruska-Hageman, A. M., Price, M. P., Nolan, B. C., Yoder, P. G., Lamani, E., Hoshi, T., Freeman, J. H., Jr., and Welsh, M. J. (2002) The acid-activated ion channel ASIC contributes to synaptic plasticity, learning, and memory. *Neuron* **34,** 463–477
12. Wemmie, J. A., Askwith, C. C., Lamani, E., Cassell, M. D., Freeman, J. H., Jr., and Welsh, M. J. (2003) Acid-sensing ion channel 1 is localized in brain regions with high synaptic density and contributes to fear conditioning. *J. Neurosci.* **23,** 5496–5502
13. Coryell, M. W., Wunsch, A. M., Haenfler, J. M., Allen, J. E., McBride, J. L., Davidson, B. L., and Wemmie, J. A. (2008) Restoring acid-sensing ion channel-1a in the amygdala of knock-out mice rescues fear memory but not unconditioned fear responses. *J. Neurosci.* **28,** 13738–13741
14. Ziemann, A. E., Allen, J. E., Dahdaleh, N. S., Drebot, I. I., Coryell, M. W., Wunsch, A. M., Lynch, C. M., Faraci, F. M., Howard, M. A., 3rd, Welsh, M. J., and Wemmie, J. A. (2009) The amygdala is a chemosensor that detects carbon dioxide and acidosis to elicit fear behavior. *Cell* **139,** 1012–1021
15. Xiong, Z. G., Zhu, X. M., Chu, X. P., Minami, M., Hey, J., Wei, W. L., MacDonald, J. F., Wemmie, J. A., Price, M. P., Welsh, M. J., and Simon, R. P. (2004) Neuroprotection in ischemia: blocking calcium-permeable acid-sensing ion channels. *Cell* **118,** 687–698
16. Friese, M. A., Craner, M. J., Etzensperger, R., Vergo, S., Wemmie, J. A., Welsh, M. J., Vincent, A., and Fugger, L. (2007) Acid-sensing ion channel-1 contributes to axonal degeneration in autoimmune inflammation of the central nervous system. *Nat. Med.* **13,** 1483–1489
17. Wong, H. K., Bauer, P. O., Kurosawa, M., Goswami, A., Washizu, C., Machida, Y., Tosaki, A., Yamada, M., Knöpfel, T., Nakamura, T., and Nukina, N. (2008) Blocking acid-sensing ion channel 1 alleviates Huntington's disease pathology via an ubiquitin-proteasome system-dependent mechanism. *Hum. Mol. Genet.* **17,** 3223–3235
18. Arias, R. L., Sung, M. L., Vasylyev, D., Zhang, M. Y., Albinson, K., Kubek, K., Kagan, N., Beyer, C., Lin, Q., Dwyer, J. M., Zaleska, M. M., Bowlby, M. R., Dunlop, J., and Monaghan, M. (2008) Amiloride is neuroprotective in an MPTP model of Parkinson's disease. *Neurobiol. Dis.* **31,** 334–341
19. Hu, R., Duan, B., Wang, D., Yu, Y., Li, W., Luo, H., Lu, P., Lin, J., Zhu, G., Wan, Q., and Feng, H. (2011) Role of acid-sensing ion channel 1a in the secondary damage of traumatic spinal cord injury. *Ann. Surg.* **254,** 353–362
20. Yu, Y., Chen, Z., Li, W. G., Cao, H., Feng, E. G., Yu, F., Liu, H., Jiang, H., and Xu, T. L. (2010) A nonproton ligand sensor in the acid-sensing ion channel. *Neuron* **68,** 61–72
21. Bohlen, C. J., Chesler, A. T., Sharif-Naeini, R., Medzihradszky, K. F., Zhou, S., King, D., Sánchez, E. E., Burlingame, A. L., Basbaum, A. I., and Julius, D. (2011) A heteromeric Texas coral snake toxin targets acid-sensing ion channels to produce pain. *Nature* **479,** 410–414
22. Diochot, S., Baron, A., Salinas, M., Douguet, D., Scarzello, S., Dabert-Gay, A. S., Debayle, D., Friend, V., Alloui, A., Lazdunski, M., and Lingueglia, E. (2012) Black mamba venom peptides target acid-sensing ion channels to abolish pain. *Nature* **490,** 552–555
23. Mazzuca, M., Heurteaux, C., Alloui, A., Diochot, S., Baron, A., Voilley, N., Blondeau, N., Escoubas, P., Gélot, A., Cupo, A., Zimmer, A., Zimmer, A. M., Eschalier, A., and Lazdunski, M. (2007) A tarantula peptide against pain via ASIC1a channels and opioid mechanisms. *Nat. Neurosci.* **10,** 943–945
24. Duan, B., Wu, L. J., Yu, Y. Q., Ding, Y., Jing, L., Xu, L., Chen, J., and Xu, T. L. (2007) Upregulation of acid-sensing ion channel ASIC1a in spinal dorsal horn neurons contributes to inflammatory pain hypersensitivity. *J. Neurosci.* **27,** 11139–11148
25. Escoubas, P., De Weille, J. R., Lecoq, A., Diochot, S., Waldmann, R., Champigny, G., Moinier, D., Ménez, A., and Lazdunski, M. (2000) Isolation of a tarantula toxin specific for a class of proton-gated Na^+ channels. *J. Biol. Chem.* **275,** 25116–25121
26. Benson, C. J., Xie, J., Wemmie, J. A., Price, M. P., Henss, J. M., Welsh, M. J., and Snyder, P. M. (2002) Heteromultimers of DEG/ENaC subunits form H^+-gated channels in mouse sensory neurons. *Proc. Natl. Acad. Sci. U.S.A.* **99,** 2338–2343
27. Weng, J. Y., Lin, Y. C., and Lien, C. C. (2010) Cell type-specific expression of acid-sensing ion channels in hippocampal interneurons. *J. Neurosci.* **30,** 6548–6558
28. Duan, B., Wang, Y. Z., Yang, T., Chu, X. P., Yu, Y., Huang, Y., Cao, H., Hansen, J., Simon, R. P., Zhu, M. X., Xiong, Z. G., and Xu, T. L. (2011) Extracellular spermine exacerbates ischemic neuronal injury through sensitization of ASIC1a channels to extracellular acidosis. *J. Neurosci.* **31,** 2101–2112
29. Gautam, M., and Benson, C. J. (2013) Acid-sensing ion channels (ASICs) in mouse skeletal muscle afferents are heteromers composed of ASIC1a, ASIC2, and ASIC3 subunits. *FASEB J.* **27,** 793–802
30. Jasti, J., Furukawa, H., Gonzales, E. B., and Gouaux, E. (2007) Structure of acid-sensing ion channel 1 at 1.9 A resolution and low pH. *Nature* **449,** 316–323
31. Baconguis, I., and Gouaux, E. (2012) Structural plasticity and dynamic selectivity of acid-sensing ion channel-spider toxin complexes. *Nature* **489,** 400–405
32. Dawson, R. J., Benz, J., Stohler, P., Tetaz, T., Joseph, C., Huber, S., Schmid, G., Hügin, D., Pflimlin, P., Trube, G., Rudolph, M. G., Hennig, M., and Ruf, A. (2012) Structure of the acid-sensing ion channel 1 in complex with the gating modifier Psalmotoxin 1. *Nat. Commun.* **3,** 936
33. Baconguis, I., Bohlen, C. J., Goehring, A., Julius, D., and Gouaux, E. (2014) X-ray structure of acid-sensing ion channel 1-snake toxin complex reveals open state of a Na^+-selective channel. *Cell* **156,** 717–729
34. Chen, X., Kalbacher, H., and Gründer, S. (2006) Interaction of acid-sensing ion channel (ASIC) 1 with the tarantula toxin psalmotoxin 1 is state dependent. *J. Gen. Physiol.* **127,** 267–276
35. Passero, C. J., Okumura, S., and Carattino, M. D. (2009) Conformational changes associated with proton-dependent gating of ASIC1a. *J. Biol. Chem.* **284,** 36473–36481
36. Tolino, L. A., Okumura, S., Kashlan, O. B., and Carattino, M. D. (2011) Insights into the mechanism of pore opening of acid-sensing ion channel 1a. *J. Biol. Chem.* **286,** 16297–16307
37. Kusama, N., Gautam, M., Harding, A. M., Snyder, P. M., and Benson, C. J. (2013) Acid-sensing ion channels (ASICs) are differentially modulated by anions dependent upon their subunit composition. *Am. J. Physiol. Cell Physiol.* **304,** C89–C101
38. Kusama, N., Harding, A. M., and Benson, C. J. (2010) Extracellular chloride modulates the desensitization kinetics of acid-sensing ion channel 1a (ASIC1a). *J. Biol. Chem.* **285,** 17425–17431
39. Karlin, A., and Akabas, M. H. (1998) Substituted-cysteine accessibility

method. *Methods Enzymol.* **293,** 123–145
40. Passero, C. J., Carattino, M. D., Kashlan, O. B., Myerburg, M. M., Hughey, R. P., and Kleyman, T. R. (2010) Defining an inhibitory domain in the γ subunit of the epithelial sodium channel. *Am. J. Physiol. Renal Physiol.* **299,** F854–861
41. Guex, N., and Peitsch, M. C. (1997) SWISS-MODEL and the Swiss-Pdb-Viewer: an environment for comparative protein modeling. *Electrophoresis* **18,** 2714–2723
42. Krauson, A. J., Rued, A. C., and Carattino, M. D. (2013) Independent contribution of extracellular proton binding sites to ASIC1a activation. *J. Biol. Chem.* **288,** 34375–34383
43. Gonzales, E. B., Kawate, T., and Gouaux, E. (2009) Pore architecture and ion sites in acid-sensing ion channels and P2X receptors. *Nature* **460,** 599–604
44. Li, T., Yang, Y., and Canessa, C. M. (2009) Interaction of the aromatics Tyr-72/Trp-288 in the interface of the extracellular and transmembrane domains is essential for proton gating of acid-sensing ion channels. *J. Biol. Chem.* **284,** 4689–4694
45. Ramaswamy, S. S., MacLean, D. M., Gorfe, A. A., and Jayaraman, V. (2013) Proton-mediated conformational changes in an acid-sensing ion channel. *J. Biol. Chem.* **288,** 35896–35903
46. Della Vecchia, M. C., Rued, A. C., and Carattino, M. D. (2013) Gating transitions in the palm domain of ASIC1a. *J. Biol. Chem.* **288,** 5487–5495
47. Langlhofer, G., Janzen, D., Meiselbach, H., and Villmann, C. (2015) Length of the TM3–4 loop of the glycine receptor modulates receptor desensitization. *Neurosci. Lett.* **600,** 176–181
48. Gielen, M., Thomas, P., and Smart, T. G. (2015) The desensitization gate of inhibitory Cys-loop receptors. *Nat. Commun.* **6,** 6829
49. Meiselbach, H., Vogel, N., Langlhofer, G., Stangl, S., Schleyer, B., Bahnassawy, L., Sticht, H., Breitinger, H. G., Becker, C. M., and Villmann, C. (2014) Single expressed glycine receptor domains reconstitute functional ion channels without subunit-specific desensitization behavior. *J. Biol. Chem.* **289,** 29135–29147
50. McKinnon, N. K., Bali, M., and Akabas, M. H. (2012) Length and amino acid sequence of peptides substituted for the 5-HT3A receptor M3M4 loop may affect channel expression and desensitization. *PLoS ONE* **7,** e35563
51. Zhang, J., Xue, F., Liu, Y., Yang, H., and Wang, X. (2013) The structural mechanism of the Cys-loop receptor desensitization. *Mol. Neurobiol.* **48,** 97–108
52. Cushman, K. A., Marsh-Haffner, J., Adelman, J. P., and McCleskey, E. W. (2007) A conformation change in the extracellular domain that accompanies desensitization of acid-sensing ion channel (ASIC) 3. *J. Gen. Physiol.* **129,** 345–350
53. Li, T., Yang, Y., and Canessa, C. M. (2010) Asn-415 in the β11-β12 linker decreases proton-dependent desensitization of ASIC1. *J. Biol. Chem.* **285,** 31285–31291
54. Frey, E. N., Pavlovicz, R. E., Wegman, C. J., Li, C., and Askwith, C. C. (2013) Conformational changes in the lower palm domain of ASIC1a contribute to desensitization and RFamide modulation. *PLoS ONE* **8,** e71733
55. Roy, S., Boiteux, C., Alijevic, O., Liang, C., Bernèche, S., and Kellenberger, S. (2013) Molecular determinants of desensitization in an ENaC/degenerin channel. *FASEB J.* **27,** 5034–5045
56. Bonifacio, G., Lelli, C. I., and Kellenberger, S. (2014) Protonation controls ASIC1a activity via coordinated movements in multiple domains. *J. Gen. Physiol.* **143,** 105–118